

Supplementary Information

Cooperation and competition of halogen bonding and van der Waals force in a supramolecular engineering at the aliphatic hydrocarbon/graphite interface: position and number of bromine group effects

Bao Zha, Meiqiu Dong, Xinrui Miao, Shan Peng, Yican Wu, Kai Miao, Yi Hu and
Wenli Deng**

College of Materials Science and Engineering, South China University of
Technology, Guangzhou 510640, China

E-mail Address: msxrmiao@scut.edu.cn, wldeng@scut.edu.cn

Corresponding author: College of Materials Science and Engineering

South China University of Technology,

Wushan Road, Tianhe District, Guangzhou 510640, P. R.

China.

Tel: (+86)020-22236708

E-mail: msxrmiao@scut.edu.cn; wldeng@scut.edu.cn

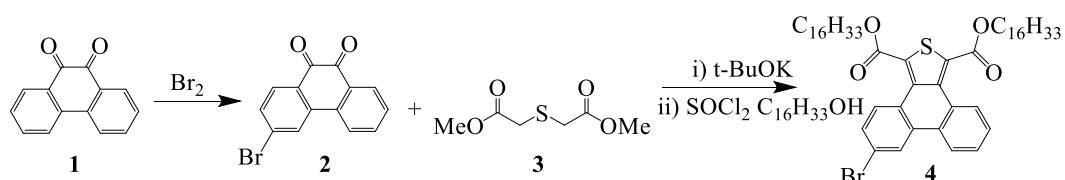
Experimental Section

1. General Information

^1H spectra were recorded out on a Bruker AV-600 MHz NMR spectrometer.

2. Synthesis and Characterization of (4) 6-DBTD

2.1. Scheme 1. Compound 4



3-Bromo-9,10-phenanthrenequinone **2**, and acetic acid, 2,2'-thiobis-1,1'-dimethyl ester **3** were synthesized as previously reported in the literature.¹⁻³

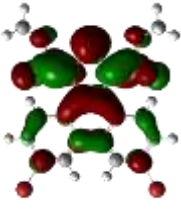
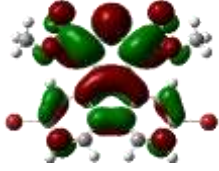
Compound 4 3-bromo-9,10-phenanthrenequinone **2** (2.87 g, 10 mmol) and **3** (2.14 g, 12 mmol) were transferred to a dry 500 mL round-bottom flask and then dissolved in benzene (200 mL) under an atmosphere of nitrogen. After gradually adding a solution of t-BuOK (5.6 g, 50 mmol) in methanol (30 mL), the green dark brown suspension was stirred at room temperature for 5 days. The reaction mixture was poured into H₂O (150 mL) and the organic solvent was removed under reduced pressure. Washing the product with HCl (aq, 10%) is to give a yellow solid. Thereafter, the yellow solid was dissolved in SOCl₂ (15 mL) and the reddish-colored reaction mixture was stirred at 80 °C for 6 h. The SOCl₂ was removed under reduced pressure. *n*-Hexadecanol (4.85 g, 20 mmol) and THF (30 mL) were added to the mixture, which was stirred at 100 °C for another 2 h. The solvent was removed by vacuum. The crude product was subjected to column chromatography (Silical gel 20% EA/PE) to give **4** as a solid.

Data for 4. ^1H NMR (600 MHz, CDCl₃, ppm): δ 8.87 (1H, m), 8.85 (1H, m), 8.59 (1H, m), 8.40 (1H, m), 7.65 (1H, m), 7.64 (1H, m), 7.58 (1H, m), 4.47 (4H, m), 1.85 (4H, m), 1.59 (4H, m), 1.28 (48H, m), 0.90 (6H, m).

Notes and references

1. N. Fomina, S. E. Bradforth and T. E. Hogen-Esch, *Macromolecules*, 2009, **42**, 6440–6447.
2. M. Kim, J. Yoo, H. Im and J. Kim, *Synth. Met.*, 2012, **162**, 2361–2369.
3. I. Nagao, M. Shimizu and T. Hiyama, *Angew. Chem. Int. Ed.*, 2009, **48**, 7573–7576.
4. T. T. T. Bui, S. Dahaoui, C. Lecomte, G. R. Desiraju and E. Espinosa, *Angew. Chem. Int. Ed.*, 2009, **48**, 3838–3841.

Table S1 Calculated frontier molecular orbitals (MOs) of the 6,9-DBTD and 5,10-DBTD from DFT calculations.

Compounds	HOMO	LUMO
6,9-DBTD		
5,10-DBTD		

(1) Self-assembled structures at the aliphatic solvent/graphite interface

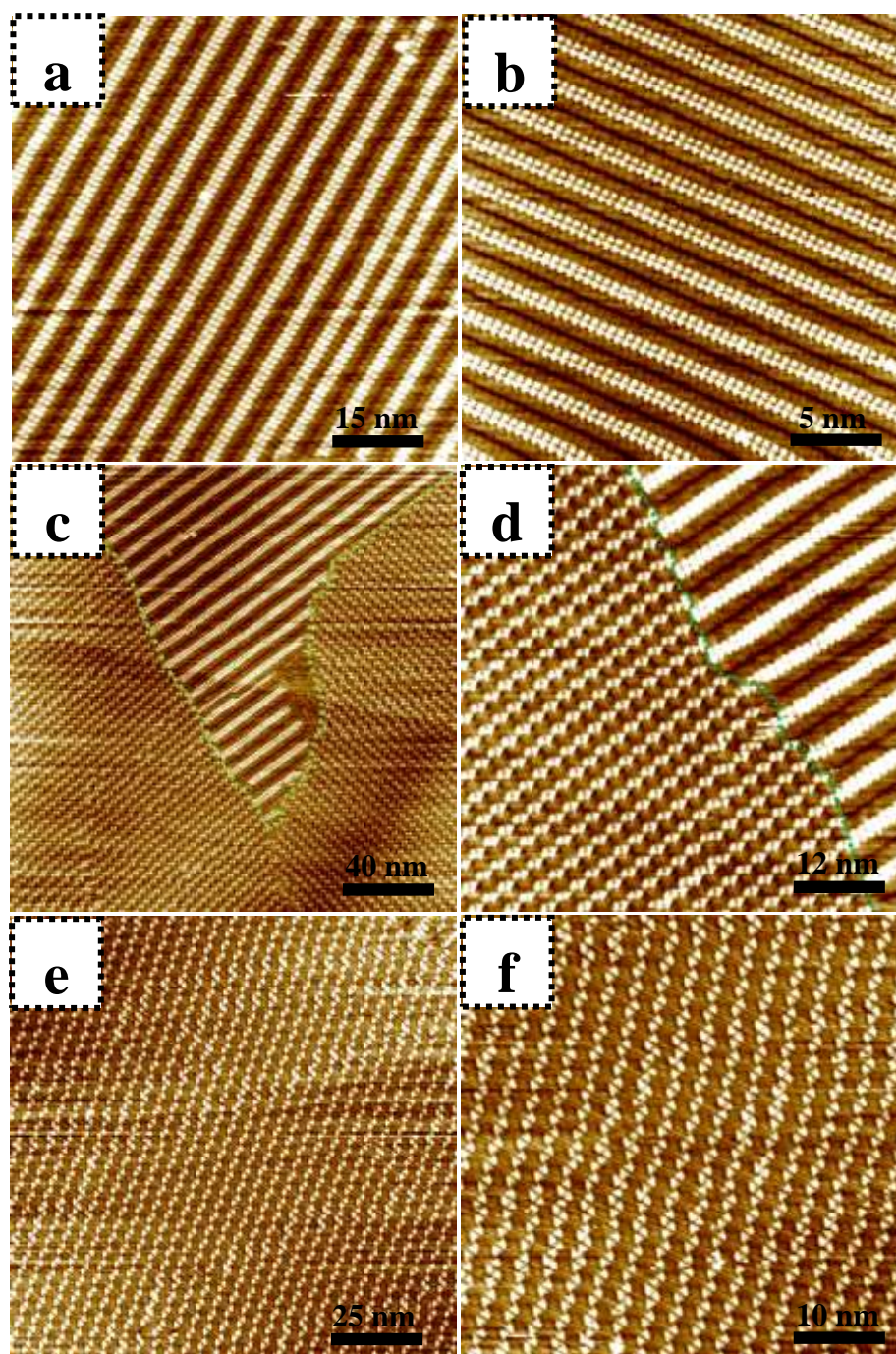


Fig. S1 Large-scale STM images of 6,9-DBTD self-assembly in *n*-tridecane on the HOPG surface. (a, b) Lamellar structure ($7.9 \times 10^{-3} - 9.6 \times 10^{-4}$ M). $I_t = 426$ pA and $V_{\text{bias}} = 669$ mV. (c, d) Coexistence of lamellar structure and coadsorbed linear structure ($7.5 \times 10^{-4} - 1.6 \times 10^{-5}$ M). $I_t = 428$ pA and $V_{\text{bias}} = 673$ mV. (e, f) Coadsorbed linear structure ($9.6 \times 10^{-4} - 6.5 \times 10^{-6}$ M). $I_t = 421$ pA and $V_{\text{bias}} = 671$ mV.

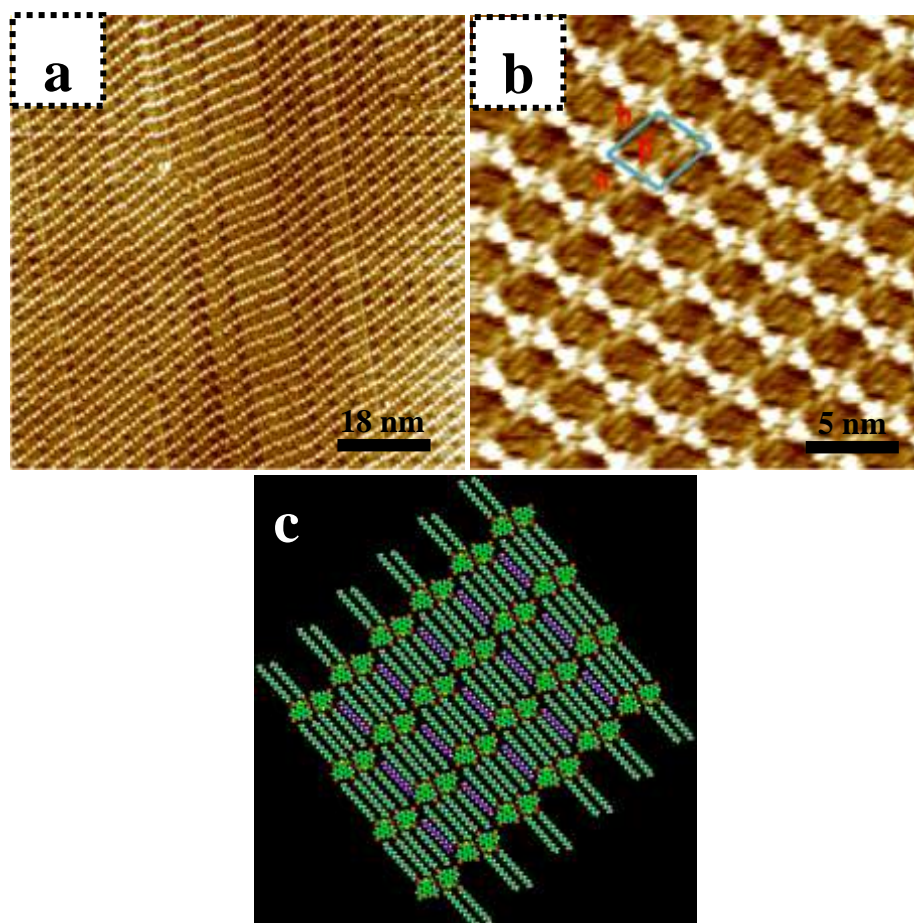


Fig. S2 (a, b) Large-scale and high-resolution STM images of 6,9-DBTD self-assembly at the *n*-tetradecane/HOPG interface. $I_t = 412$ pA and $V_{\text{bias}} = 672$ mV. (c) Molecular model corresponds to the self-assembled structure.

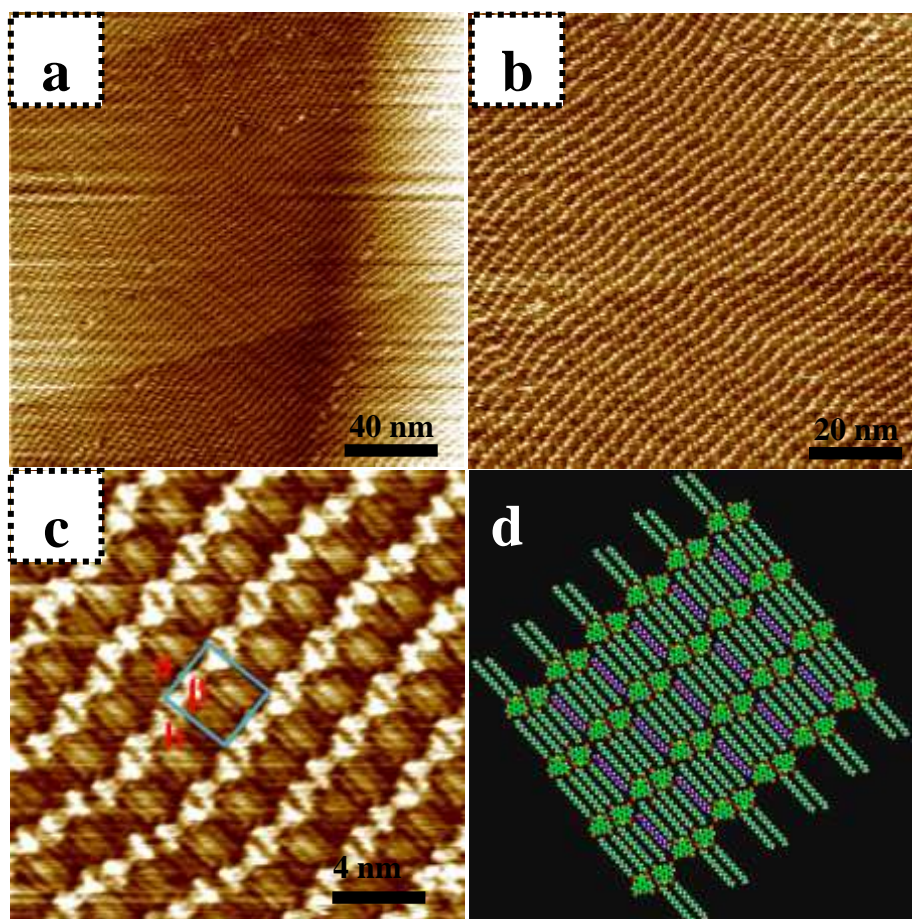


Fig. S3 (a–c) Large-scale, small-scale and high-resolution STM images of 6,9-DBTD self-assembly at the *n*-pentadecane/HOPG interface. $I_t = 412$ pA and $V_{\text{bias}} = 672$ mV. (d) Molecular model corresponds to the self-assembled structure.

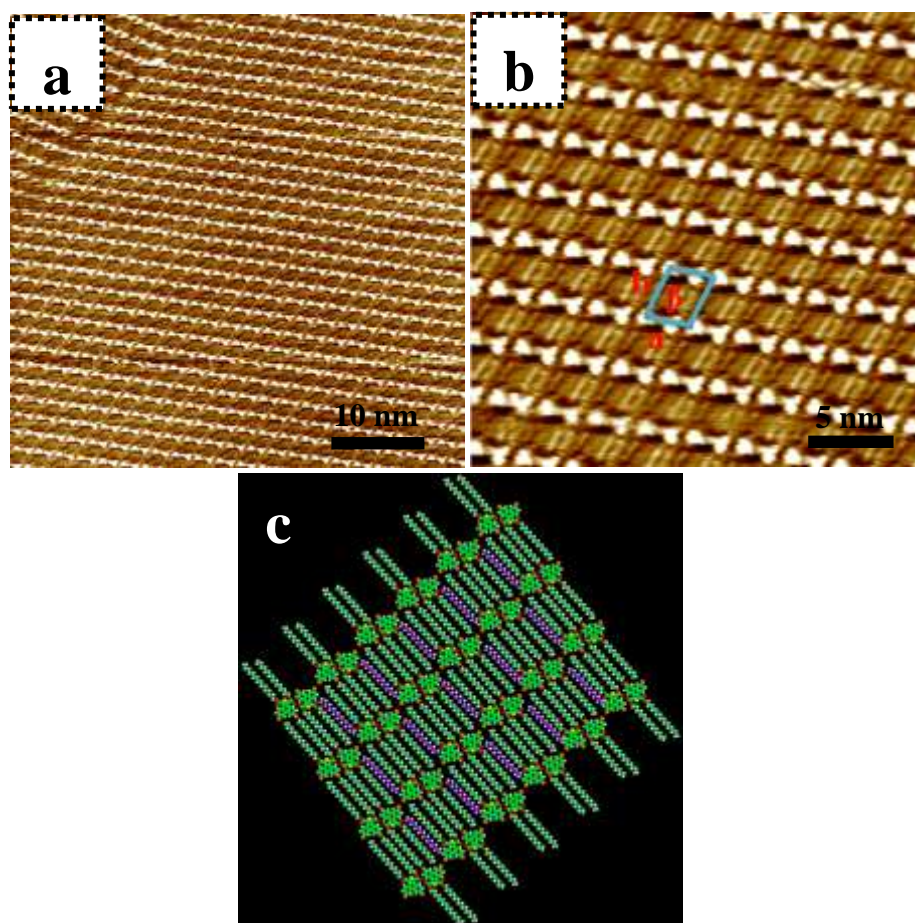


Fig. S4 (a, b) Large-scale and high-resolution STM images of 6,9-DBTD self-assembly at the *n*-hexadecane/HOPG interface. $I_t = 426$ pA and $V_{\text{bias}} = 667$ mV. (c) Molecular model corresponds to the self-assembled structure.

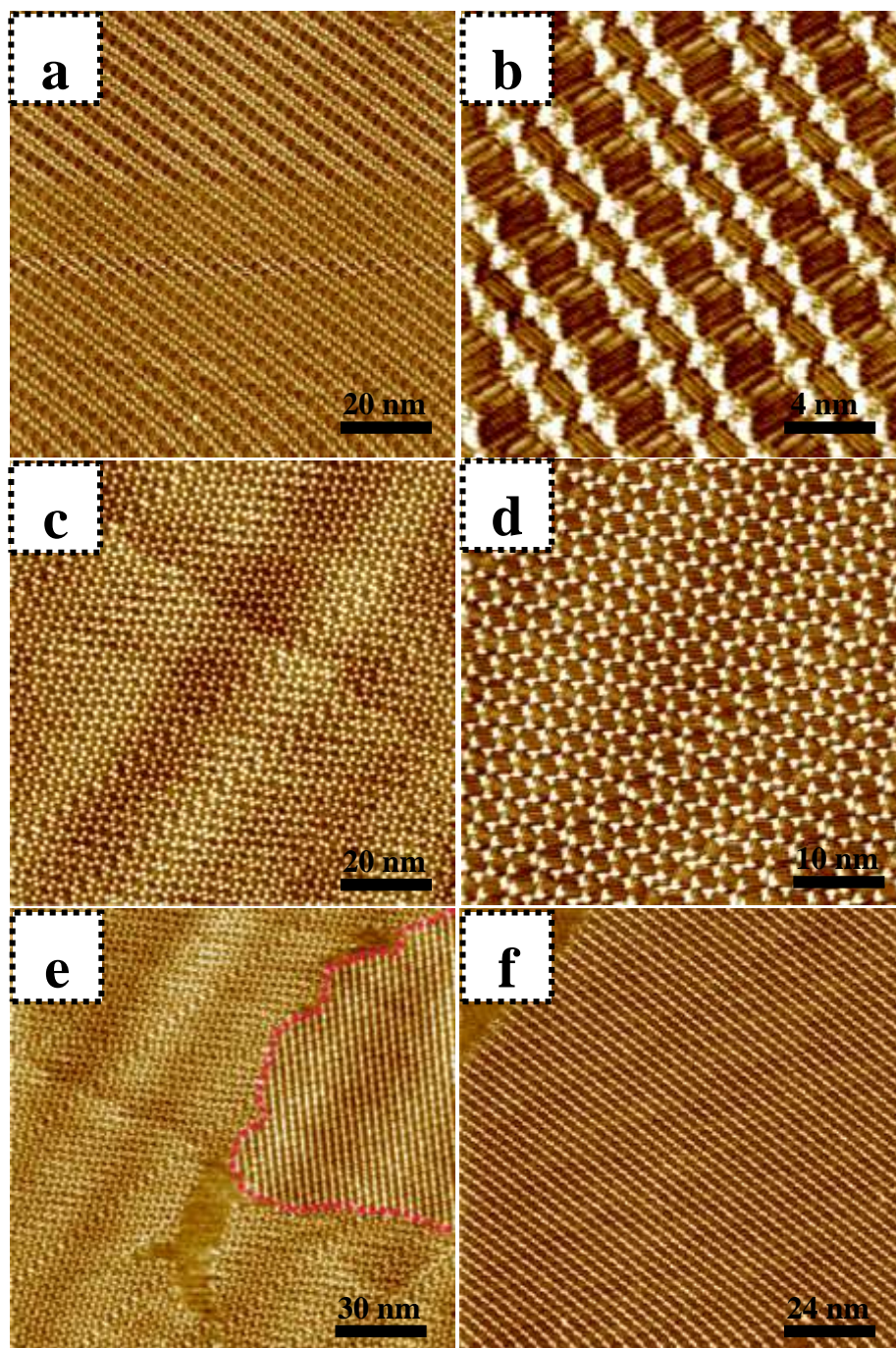


Fig. S5 (a, b) Large-scale and high-resolution STM images of 5,10-DBTD self-assembly in *n*-tridecane with high concentrations ($8.1 \times 10^{-3} - 4.6 \times 10^{-4}$ M) on the HOPG surface. $I_t = 430$ pA and $V_{\text{bias}} = 655$ mV. (c, d) Large-scale and small-scale STM images of the hexagonal network pattern in *n*-tetradecane with mediate concentrations ($4.6 \times 10^{-4} - 6.8 \times 10^{-5}$ M) on the HOPG surface. $I_t = 432$ pA and $V_{\text{bias}} = 658$ mV. (e) Coexistence of hexagonal network pattern and linear pattern ($5.7 \times 10^{-5} - 8.2 \times 10^{-5}$ M). $I_t = 422$ pA and $V_{\text{bias}} = 672$ mV. (f) Linear pattern ($6.8 \times 10^{-5} - 7.0 \times 10^{-6}$ M). $I_t = 431$ pA and $V_{\text{bias}} = 651$ mV.

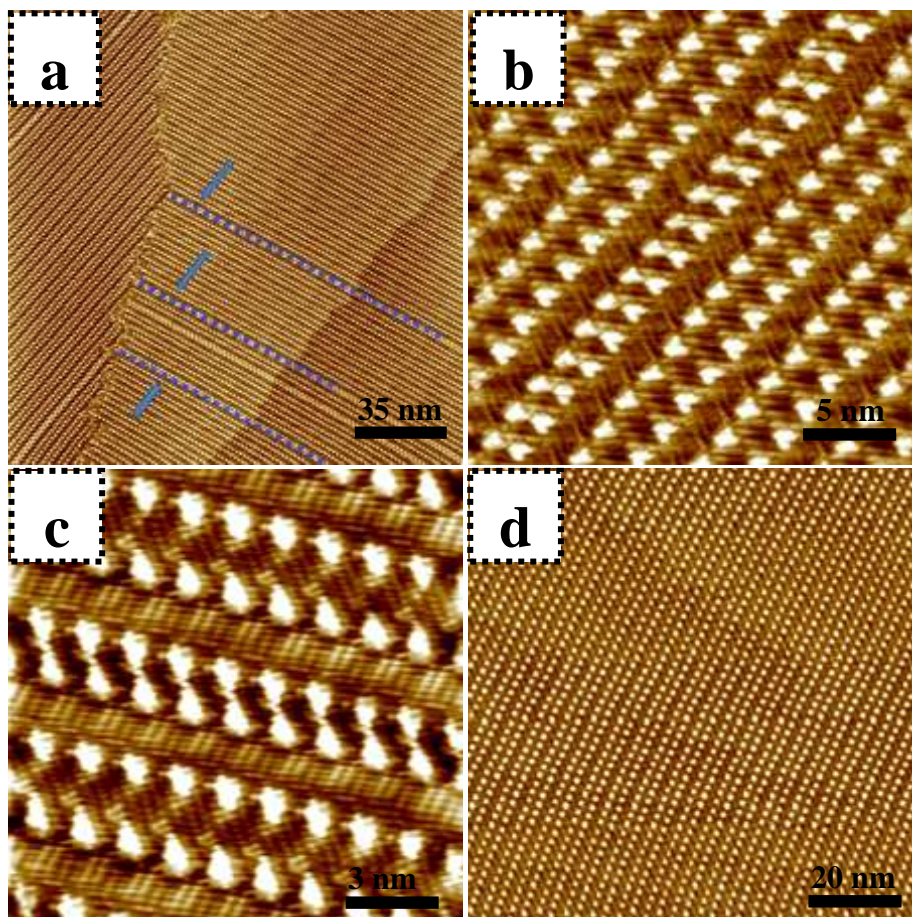


Fig. S6 (a-c) Large-scale, small-scale and high-resolution STM images of 5,10-DBTD self-assembly at the *n*-tetradecane/HOPG interface: transitional pattern in *n*-tetradecane with a medium concentrations ($7.1 \times 10^{-4} - 5.3 \times 10^{-5}$ M) on the HOPG surface. $I_t = 422$ pA and $V_{\text{bias}} = 676$ mV. (d) Large-scale STM image of 5,10-DBTD self-assembly in *n*-tetradecane with low concentrations ($5.3 \times 10^{-5} - 7.2 \times 10^{-6}$ M). $I_t = 422$ pA and $V_{\text{bias}} = 667$ mV.

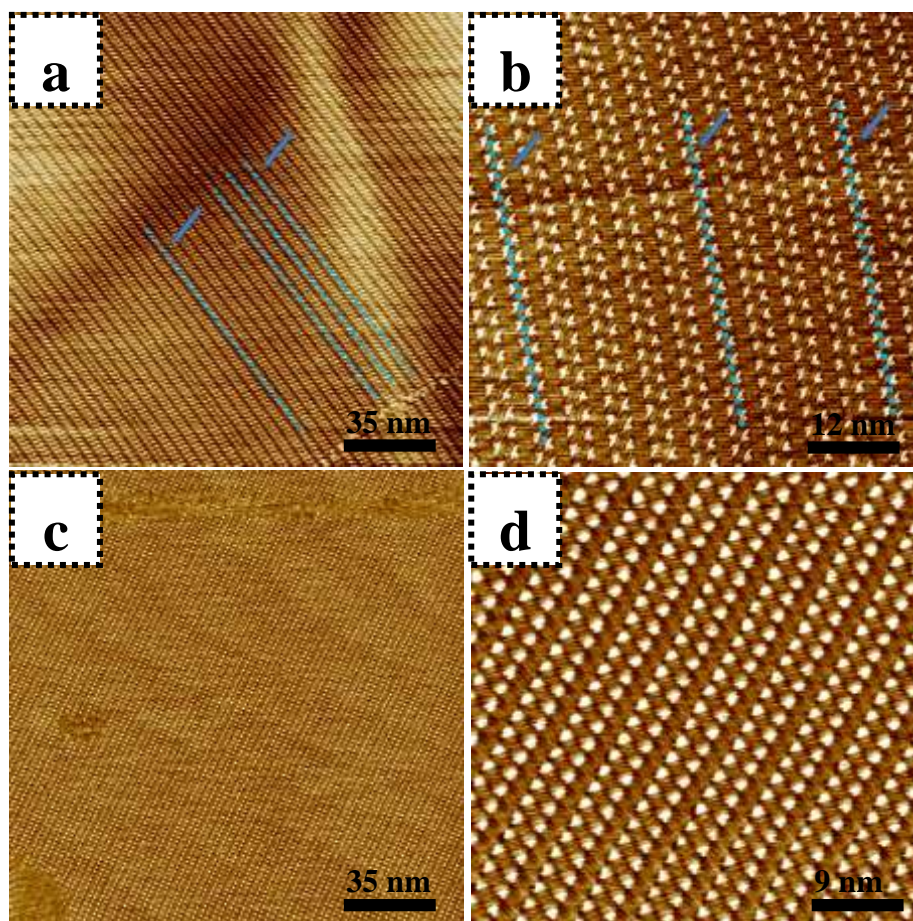


Fig. S7 (a, b) Large-scale and small-scale STM images of 5,10-DBTD self-assembly at the *n*-pentadecane/HOPG interface: transitional pattern in *n*-pentadecane with high concentrations ($6.7 \times 10^{-3} - 4.1 \times 10^{-5}$ M) on the HOPG surface. $I_t = 422$ pA and $V_{\text{bias}} = 676$ mV. (c, d) Large-scale and small-scale STM images of 5,10-DBTD self-assembly in *n*-pentadecane with low concentrations ($4.1 \times 10^{-5} - 6.9 \times 10^{-6}$ M). $I_t = 422$ pA and $V_{\text{bias}} = 667$ mV.

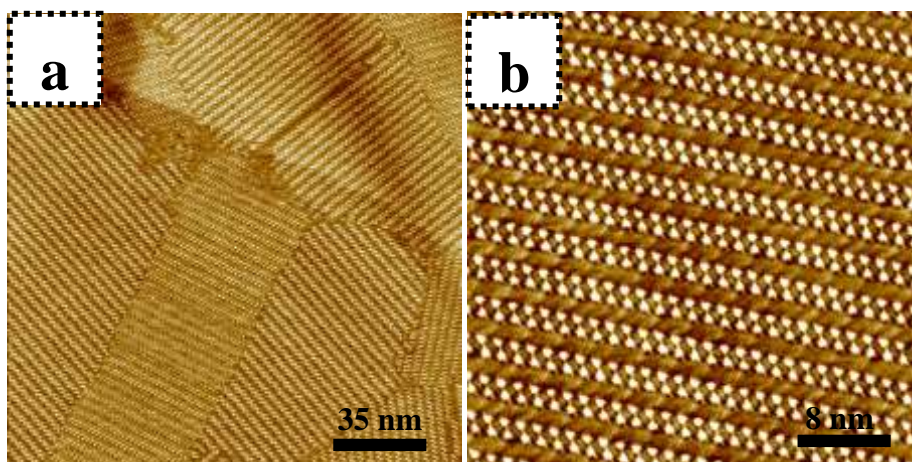


Fig. S8 (a, b) Large-scale and small-scale STM images of 5,10-DBTD self-assembly in *n*-hexadecane on the HOPG surface. $I_t = 422$ pA and $V_{\text{bias}} = 667$ mV.

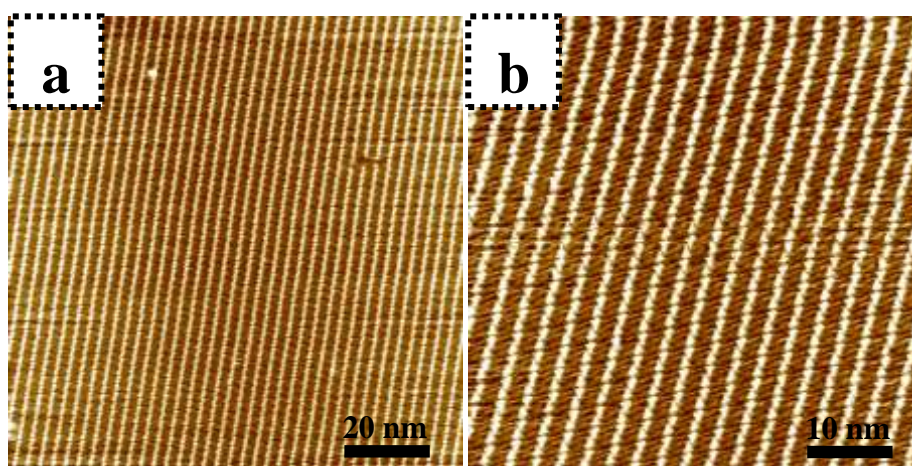
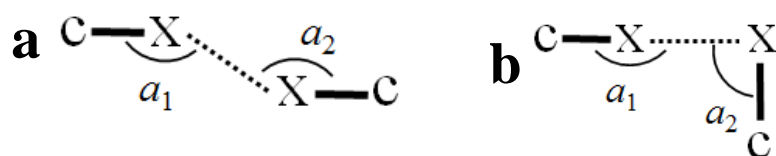


Fig. S9 (a, b) Large-scale and small-scale STM images of 6-DBTD self-assembly at the liquid/solid interface. $I_t = 427$ pA and $V_{\text{bias}} = 665$ mV.

(2) DFT Calculations for the halogen bonding

It is worth noting that two different types of X-bonds are previously classified based on the geometrical C–Br···Br angles α_1 and α_2 . Type-I interactions belong to the vdW type, which are usually connected with crystallographic inversion center. Type-II interactions can be understood as attractive interactions between the positive polar region along the X–C axis and the negative equatorial region perpendicular to the X–C axis. Type-II interactions are commonly associated with crystallographic screw axes and glide planes.⁴



Scheme S1. X-bond interaction. (a) Type-I interactions ($\alpha_1 \approx \alpha_2$). (b) Type-II interactions ($\alpha_1 \approx 180^\circ$, $\alpha_2 \approx 90^\circ$)

(3) Quantum theory of atoms in molecules (QTAIM) analyses of the intermolecular interactions

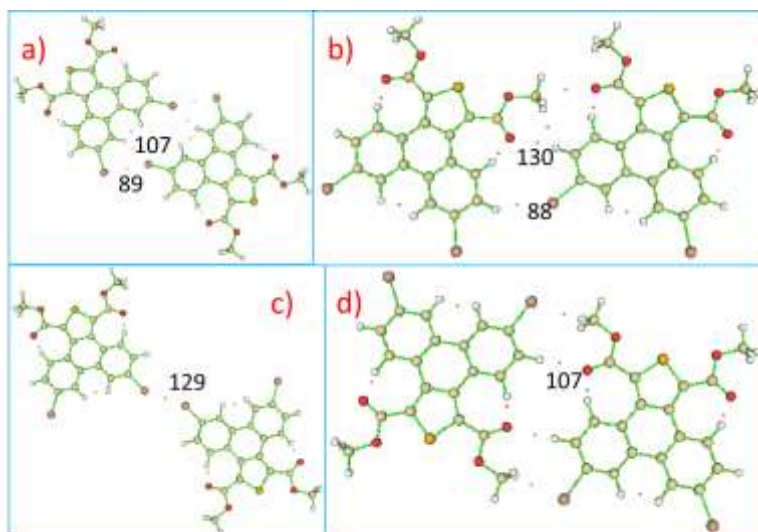


Fig. S10 Molecular graphs showing intermolecular bond critical points (BCPs, shown as small orange dots) for various molecular dimer motifs of 6,9-DBTD.

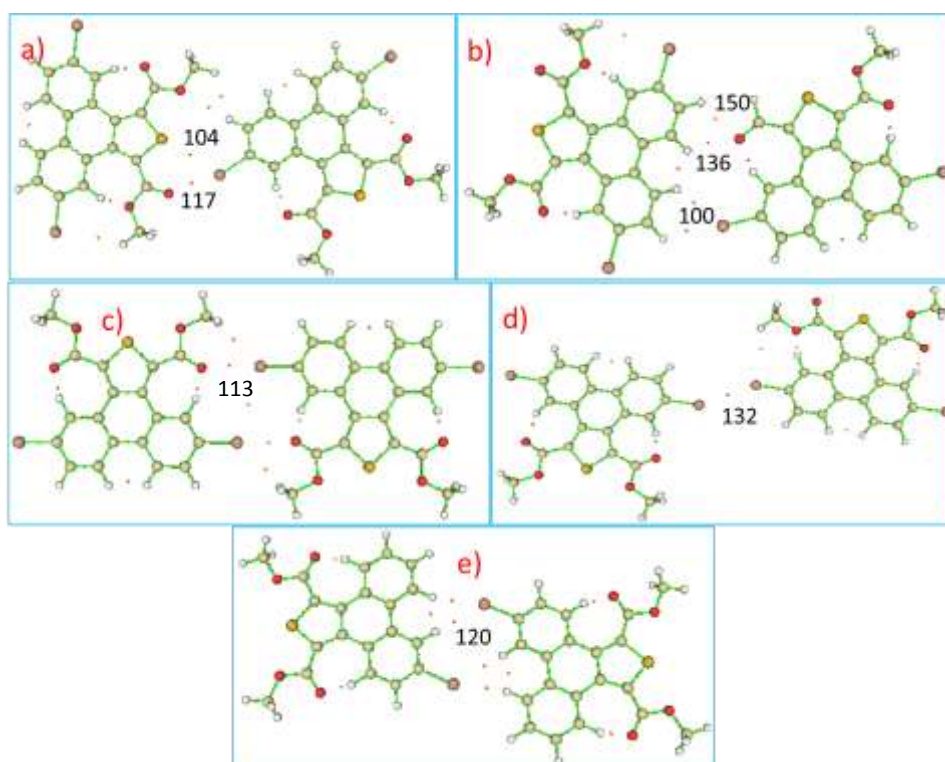


Fig. S11 Molecular graphs showing intermolecular bond critical points (BCPs, shown as small orange dots) for various molecular dimer motifs of 5,10-DBTD and 6-DBTD. (a–d) 5,10-DBTD; (e) 6-DBTD.

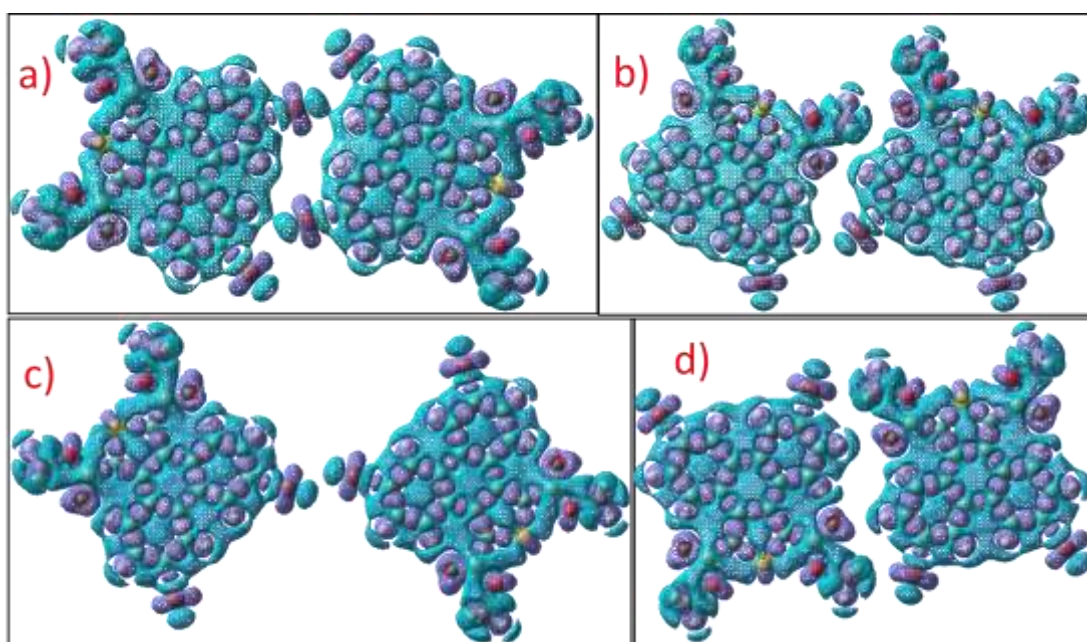


Fig. S12 (a–d) 3D deformation charge density maps in the plane four different dimers formed by 6,9-DBTD. Positive surface is shown in purple mesh, and negative surface is shown in blue mesh.

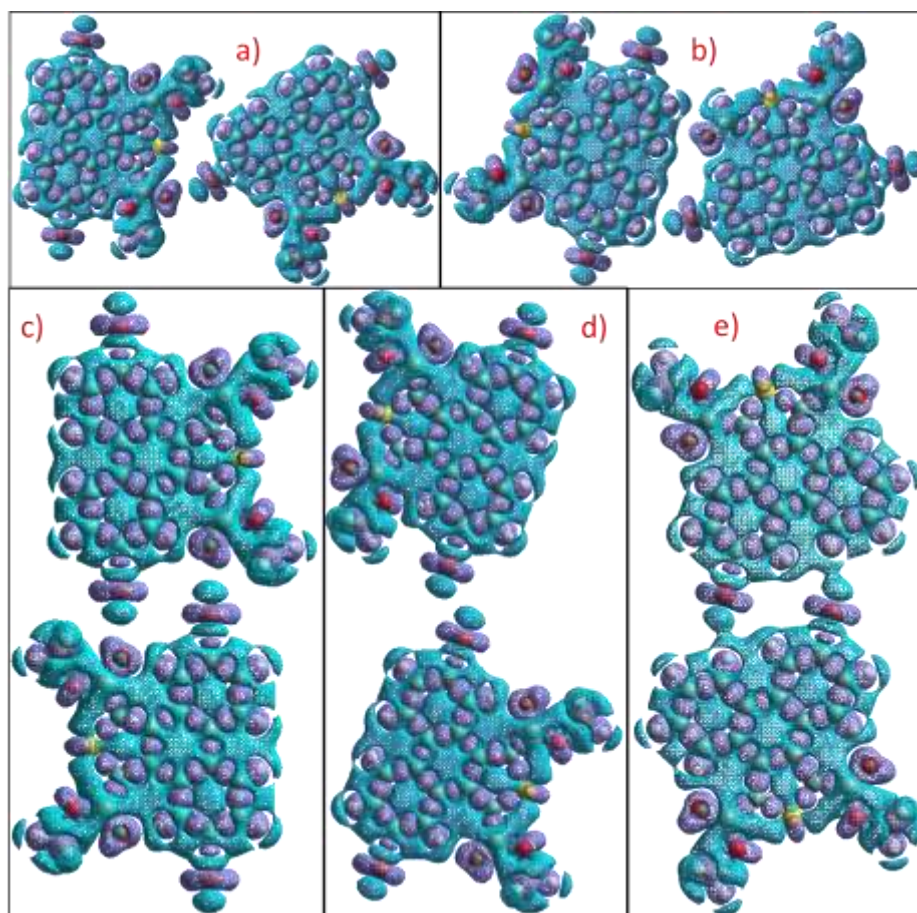


Fig. S13 (a–d) 3D deformation charge density maps in the plane four different dimers formed by 5,10-DBTD. (e) 3D deformation charge density maps in the plane four different dimers formed by 6-DBTD. Positive surface is shown in purple mesh, and negative surface is shown in blue mesh.